Mesonic Atoms: Radiative Yields of the μ-Meson K and L Series and the Effect of Meson Capture in Chemical Compounds*

MARY BETH STEARNS AND MARTIN STEARNS
Carnegie Institute of Technology, Pittsburgh, Pennsylvania
(Received November 16, 1956)

The radiative yields of the K and L series of μ-mesonic atoms have been measured for the elements $_3$Li through $_{19}$K. In the low-Z region both yield curves exhibit a rapid decrease in yield with decreasing Z. This behavior is attributed to competition between Auger and radiative transitions. However, if this is true, the Auger transition probabilities would have to be about 300 times larger than the calculated values for the $\mu-K$ yields, and about 30 times larger for the $\mu-L$ yields.

The effect of meson capture by the different elements of a compound has been measured for Al_2O_3 and CaS. For these compounds it is found to be proportional to Z within 10 to 20%, in agreement with the prediction of Fermi and Teller.

I. INTRODUCTION

THE capture process of negative mesons in condensed matter has been discussed by several authors.[1] The meson is first bound to a particular nucleus in a high quantum state ($n\simeq 15$) and then proceeds to cascade inwards toward the nucleus, transferring its energy by radiative and Auger transitions. At each intermediate level the meson can (1) be absorbed directly from the intermediate level by the nucleus, (2) make a radiative transition to a lower state and emit a quantum, or (3) make a radiationless transition to a lower state, transferring the energy difference to an atomic electron (mesonic Auger effect). If the energy difference is sufficiently large it might, alternatively, create an electron pair or excite the nucleus, but such events are highly unlikely in the light mesonic atoms discussed here.

All three processes occur and have been observed for π mesons.[2,3] In particular, nuclear absorption is exceedingly strong for pions in states of low angular momentum. A π meson in any s state will almost certainly be absorbed; absorption from the $2p$ state is practically complete for $Z\gtrsim 11$; etc. Since little is known about the pion-nucleus interaction, it necessarily complicates the study of the cascade process in π-mesonic atoms. This difficulty does not exist for μ mesons. The muon-nucleus interaction is very weak, and it is practically certain that in the course of the cascade all μ mesons reach the $1s$ state from which they are ultimately captured or in which they decay. (The cascade time is more than a million times shorter than the muon lifetime.) Accordingly, μ mesons are very useful in studying the cascade process and, in particular, the competition between radiative and Auger transitions.

* Supported by the U. S. Atomic Energy Commission.
[1] E. Fermi and E. Teller, Phys. Rev. **72**, 399 (1947); B. Ferretti, Nuovo cimento **5**, 325 (1948); J. A. Wheeler, Revs. Modern Phys. **21**, 133 (1949).
[2] Stearns, DeBenedetti, Stearns, and Leipuner, Phys. Rev. **93**, 1123 (1954).
[3] Camac, McGuire, Platt, and Schulte, Phys. Rev. **99**, 897 (1944); Camac, Halbert, and Platt, Phys. Rev. **99**, 905 (1955).

II. EXPERIMENTAL PROCEDURE

A. Experimental Setup

Figure 1 shows a plan view of the Carnegie Institute of Technology synchrocyclotron taken in the plane of the beam. The 440-Mev proton beam strikes an internal beryllium target and produces pions, some of which decay into muons in the vicinity of the target. Both pions and muons of a given momentum are focused by the fringing field of the cyclotron through an appropriate channel in the shielding wall, 12 feet thick. Outside the shielding they enter a 45° double-focusing sector magnet (of two-meter focal length) which serves both to purify the beam and focus the mesons into the counter telescope. μ mesons originating from the decay of pions during the long transit through the shielding port and beyond are largely projected out of the beam and lost.

The meson telescope and associated electronics are shown schematically in Fig. 2. Counters 1, 2, and 3 defined the incident meson beam. They consisted of stilbene crystals of square cross sections, 3 cm×3 cm, viewed by RCA 1P21 photomultipliers. The copper plus beryllium absorber between counters 2 and 3 was adjusted to make either pions or muons stop in the target. Counter 4, which was in anticoincidence with the first three counters, was usually a 1-cm thick plastic

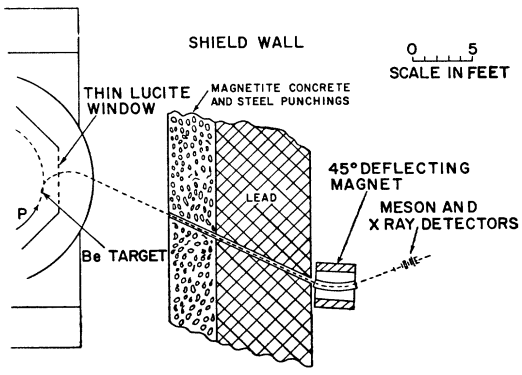

FIG. 1. Plan view of experimental arrangement.

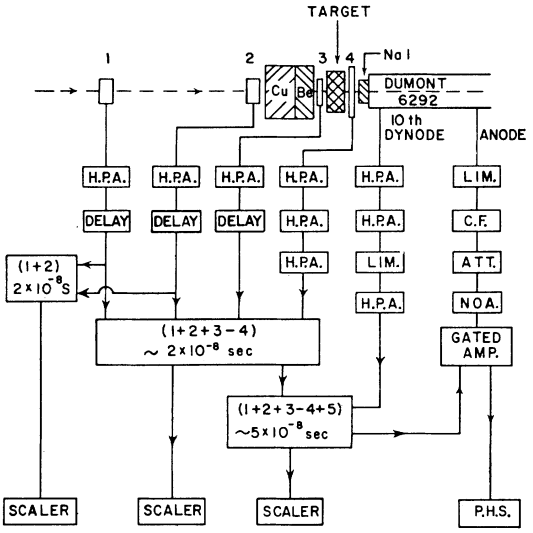

FIG. 2. Meson telescope and block diagram of associated electronics. The abbreviations are: H.P.A., Hewlett-Packard amplifier; LIM., limiter; C.F., cathode follower; ATT., attenuator; NOA., nonoverloading amplifier.

scintillator, and was viewed by an RCA 6342. It completely covered the x-ray detector, counter 5. This was a cylindrical NaI(Tl) crystal, of different size depending on the x-ray energy studied, mounted on a Dumont 6292 photomultiplier. Pulses were taken from both the anode and the last dynode of this tube. The dynode pulse was clipped hard ($\sim 2.5\times10^{-8}$ sec) and put into coincidence with the meson telescope, 1+2+3−4. A mesonic x-ray was indicated by the coincidence-anticoincidence combination 1+2+3−4+5. This opened a gated amplifier for 2 microseconds during which time it received the slow NaI anode pulse. The amplitude of the latter was then measured with a 24-channel pulse-height selector (p.h.s.).

The pulses from counters 1, 2, 3, and 4 were amplified by Hewlett-Packard wide band distributed amplifiers and then fed into a Garwin[4]-type multiple-coincidence circuit (2×10^{-8} sec). Both doubles, $D(1+2)$, and triples plus anticoincidence, $T+A.C.(1+2+3-4)$, were monitored with fast Hewlett-Packard scalers. A slower diode coincidence ($\sim 5\times10^{-8}$ sec) between one output of the $T+A.C.$ and the clipped NaI dynode pulse gave the quintuplet $Q(1+2+3-4+5)$ counting rate. The slow anode pulse from the NaI photomultiplier was amplified by a nonoverloading amplifier of the Chase-Higinbotham[5] type. The nonoverloading characteristics were very critical since x-rays of 20 to 300 kev had to be studied in the presence of pulses corresponding to ionization losses as high as 100 Mev (π^--meson stars). A diode limiter was inserted between the photomultiplier anode output and the succeeding cathode follower driver and was adjusted to attenuate all pulses due to energy losses of 1 Mev or more. Annihilation γ rays (0.511 Mev), however, were unaffected. Although the limiter was unquestionably helpful, the capacity feedthrough was sufficient to make the nonoverloading properties of the main amplifier a necessity.

The maximum $T+A.C.$ counting rate for pions was 500 counts/sec, but most runs were taken at one third this beam level in order to minimize pulse pileup in the NaI crystal. The muon beam was roughly 10% that of the pion beam. The accidental rate, determined by inserting an appropriate delay (always equal to an integral number of rf cycles) into the various arms of the coincidence-anticoincidence system, was measured to be less than 2%.

Pions and muons were cleanly separated experimentally. A differential range curve is shown in Fig. 3 where $T+A.C.$ is plotted against copper absorber thickness. (In order to reduce Coulomb scattering and the background due to star fragments, there was always an additional 1-in. thick slab of beryllium before counter 3.) The large peak is due to pions stopping in the target (and counter 3),—the smaller peak to muons. The tail at greater copper thicknesses is presumably due, for the most part, to electron contamination. By using a copper absorber thickness appropriate to the pion peak one automatically rejected all muons since their residual energy was sufficient for them to penetrate the anticoincidence counter 4. Conversely there are no pions at the muon peak. The purity of the two beams could be checked quite accurately since the

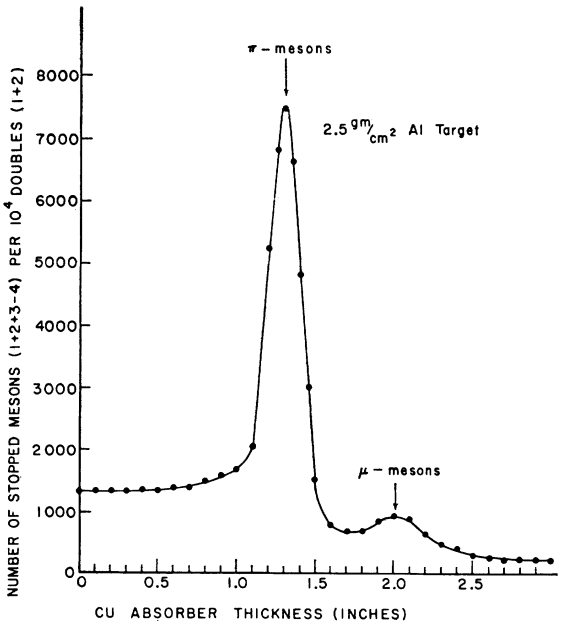

FIG. 3. Differential range curve of "110 Mev" π^- beam. In addition to the variable copper absorber thickness shown on the graph, there was always a fixed 1-in. slab of beryllium and three telescope counters in the beam.

[4] R. L. Garwin, Rev. Sci. Instr. **24**, 618 (1953).
[5] R. L. Chase and W. A. Higinbotham, Rev. Sci. Instr. **23**, 34 (1952).

mesonic x-rays themselves are a sensitive indicator of possible contamination. None was observed.

B. Targets

In all cases, with the exception of Li, Be, and B, the target material was packed uniformly inside of a thin hollow Lucite cylinder, 1 in. thick and $2\frac{3}{4}$ in. in diameter. The number of g/cm^2 of each sample was adjusted to be the same and equal to that of water. For materials of smaller density (e.g., Li and B powder), matching carbon targets of equal surface density were prepared. Likewise, Be, which was a denser rectangular slab, had its matching carbon partner.

C. NaI(Tl) Detectors

The x-ray energies of the elements investigated varied from 18 kev to about 730 kev for the $\mu-K$ series and from 25 kev to 142 kev for the $\mu-L$ series. (See Tables I and II.) In order to minimize the background counting rate, which increases roughly as the volume of the crystal, we used, in each energy region, the thinnest crystal consistent with a reasonable efficiency. For the lowest energy x-rays, up to about 60 kev, the NaI crystal was a cylinder, $1\frac{1}{2}$ in. in diameter and $\frac{1}{16}$ in. thick, and had a 5-mil aluminum window which faced the target. For the energy region from 50 kev to about 160 kev, the crystal was $1\frac{1}{2}$ in. in diameter, $\frac{1}{2}$ in. thick, and had a 25-mil aluminum window. For energies above 150 kev the NaI detector was a $1\frac{3}{4}$-in. diameter cylinder, 2 in. thick, with a 32-mil aluminum window.

D. Corrections to Yield Measurements

The raw experimental yields must be corrected for the following effects: (1) absorption and scattering of x-rays in the target, the *A.C.* counter, and the aluminum window of the NaI detector (2) escape x-rays from the NaI detector (3) carbon x-rays coming from the third counter of the meson telescope (4) x-rays from undesired elements (in the case of compounds) and contaminants (5) the variation with energy of the NaI detection efficiency.

(1) For *relative* yield determinations the correction for absorption and scattering of the mesonic x-ray in the intervening materials is quite insensitive to the direction of travel assumed for the x-ray. We have assumed, therefore, in calculating this correction, that the x-rays traverse the intervening material at an average angle of 25°. The calculation was made using absorption coefficients given in the Gladys White Tables.[6] (The absorption coefficient included photoelectric absorption, coherent scattering, and Compton scattering.) It was reasonable to assume, from the geometry, that x-rays which were scattered through an angle greater than 70° in the *A.C.* counter and 90° in the aluminum window were not detected by the NaI crystal. The effect of scattering in the meson target, particularly backscattering and inscattering, was too difficult to estimate theoretically, and was therefore studied experimentally with artificial radioactive sources. Toward this end it was first necessary to determine the effective size of the source of mesonic x-rays. It was found, by measuring the mesonic x-ray yield as a function of target size, that essentially the region of the target covered by the third counter was effective. Plane uniform radioactive sources of this size were accordingly fabricated. Measurements were taken with a given source placed at four different distances from the NaI detector, corresponding to the near face of the target, the one-third depth, the two-thirds depth, and the far face. Counting rates with bare sources in position were compared with counting rates with the sources surrounded by different target materials. In this manner the effect of absorption, inscattering, and outscattering in the various layers of the target could be studied. The sources used most extensively were Tm^{170} (84, 51 kev), RaD (47 kev), and $CePr^{144}$ (134, 34 kev). Figure 4 shows the resultant transmissions for the targets and for the *A.C.* counter plus aluminum window of each of the NaI crystals. As can be seen, the correction factor is a slowly varying function of the energy, except below 40 kev where photoelectric absorption is appreciable. Note that the transmission, for the $\mu-K$ targets, is greater than unity at low energies (low-Z targets). At these energies inscattering (including backscattering) exceeds outscattering plus photoelectric absorption. The effects are about equal at higher energies (higher-Z targets). For the $\mu-L$ targets, photoelectric absorption is dominant and the transmission is less than unity.

(2) The escape correction is important for x-ray energies not too much greater than the iodine K-edge (33.2 kev). Since x-rays in this energy region are strongly absorbed near the surface of the NaI crystal, the fluorescent iodine K-line has a considerable escape

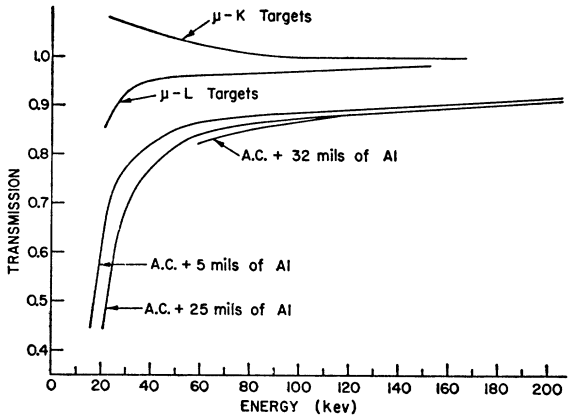

FIG. 4. Transmission corrections, as a function of x-ray energy, for the meson targets and for the anticoincidence counter plus aluminum windows of the several NaI(Tl) detectors.

[6] G. R. White, National Bureau of Standards Report 1003, 1952 (unpublished).

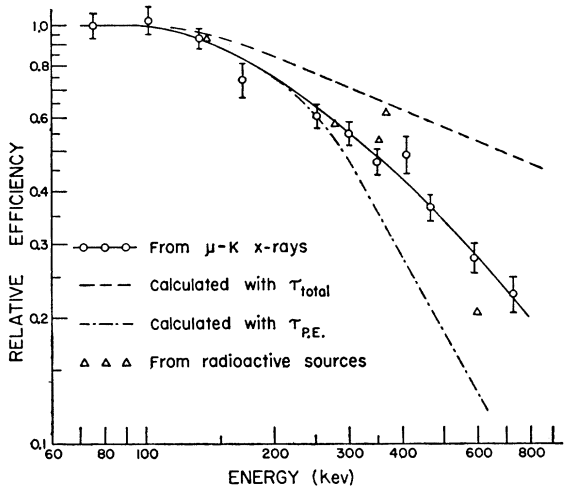

FIG. 5. Relative efficiency curves for the 2-in.×1¾-in. diameter crystal. These curves include corrections for absorption and scattering of the x-rays traversing the *A.C.* counter and the 32-mil Al window of the NaI detector. They have been arbitrarily matched at low energies.

probability and thus may not be absorbed in the crystal. We have observed several escape peaks in both π and μ spectra and have been able, in these cases, to measure this correction directly. We find that the measured corrections agree quite well with a formula given by Novey.[7] We have, therefore, used this formula generally for our escape corrections.

(3) Because of the momentum spread of the μ-meson beam, some μ mesons stop in the third counter of the meson telescope. These constitute a source of carbon K x-rays (see Figs. 6 and 8). This satellite peak is well resolved in some cases and can be subtracted off directly. In those cases where this is not possible, the third counter contribution can be estimated quite accurately by interpolation.

(4) With the exception of N, O, F, and Cl, all targets were pure elements. The nitrogen target was hydrazine $(N_2H_4)_n$ of 95% purity. A 5% water contamination was easily corrected by using the measured value of the oxygen x-ray yield. (It is well known, from the experiments of Panofsky *et al.*,[8] that the hydrogen in such compounds does not absorb mesons.) For the fluorine and chlorine measurements, targets of LiF and LiCl were used, respectively. It appears, as discussed in Sec. III-C, that the lithium in these compounds is not effective in absorbing mesons, and no corrections were made for it.

(5) The detection efficiencies of the $\frac{1}{16}$-in. and $\frac{1}{2}$-in. NaI crystals could be calculated in a straightforward manner since edge effects, for these, were negligible over the energy regions in which they were used. However, in the case of the 2-in. crystal, the efficiency variation with energy is more difficult to calculate. It was obtained in the following three ways.

The simplest and most reliable method was to use the results of the radiative $\mu-K$ yields. We assume that the $\mu-K$ yield is essentially constant over the interval $8\leqslant Z\leqslant 19$ since, for these Z's, the competing processes of Auger effect and nuclear capture are negligible. This implies that the cascade scheme does not vary drastically over this Z interval. With these assumptions the measured $\mu-K$ radiative yield, corrected for the four previously listed effects, is then a direct measure of the relative NaI efficiency. (Additional support for this method comes from measurements on π yields made with a large 3-in. diameter, 3-in. thick NaI crystal used with various sized collimators. Over the energy region where this crystal had nearly uniform efficiency the relative yields were observed to be the same as those obtained with the 2-in. crystal, corrected as described.) Figure 5 shows the efficiency curve for the 2-in. crystal (and 1-in. thick targets) obtained in this manner.

The efficiency was also measured using radioactive sources. For these measurements plane uniform sources were fabricated and placed at varying distances from the NaI detector as described above in the absorption corrections (1). The sources selected, Hg^{197}, Hg^{203}, Re^{186}, and I^{131}, had at least two γ rays with a known ratio of intensities, and these were used to obtain a relative efficiency curve. Figure 5 shows points obtained in this manner. The agreement with the first (mesonic yield) efficiency curve is fair considering the paucity of available information on the relative intensities of the γ rays.

The third method for getting the efficiency correction was by calculation. This is difficult to do reliably because of the poor geometry and edge effects. The calculation was performed by assuming a point source on the axis of the NaI detector and 2.2 cm in front of it. This corresponds to a distance one third of the way into the target. Other calculations, made with varying distances of the source, showed that the results were not very sensitive over the width of the target. The method of the calculation is described by Rietjens *et al.*[9] and takes care of edge effects caused by γ rays passing through the corners of the detector. The calculations give the efficiency in terms of an absorption coefficient, τ. In Fig. 5, the efficiency has been plotted for two extreme values of τ, τ equal to the photoelectric absorption coefficient and τ equal to the total absorption coefficient. It can be seen that the two curves bracket the efficiency determined from the μ-meson yields as would be expected.

All of the curves in Fig. 5 include the correction for scattering and absorption in the *A.C.* counter plus aluminum window.

[7] T. B. Novey, Phys. Rev. **89**, 672 (1953).
[8] Panofsky, Aamodt, and Hadley, Phys. Rev. **81**, 565 (1951).
[9] Rietjens, Arkenbout, Wolters, and Kluyver, Physica **21**, 110 (1955).

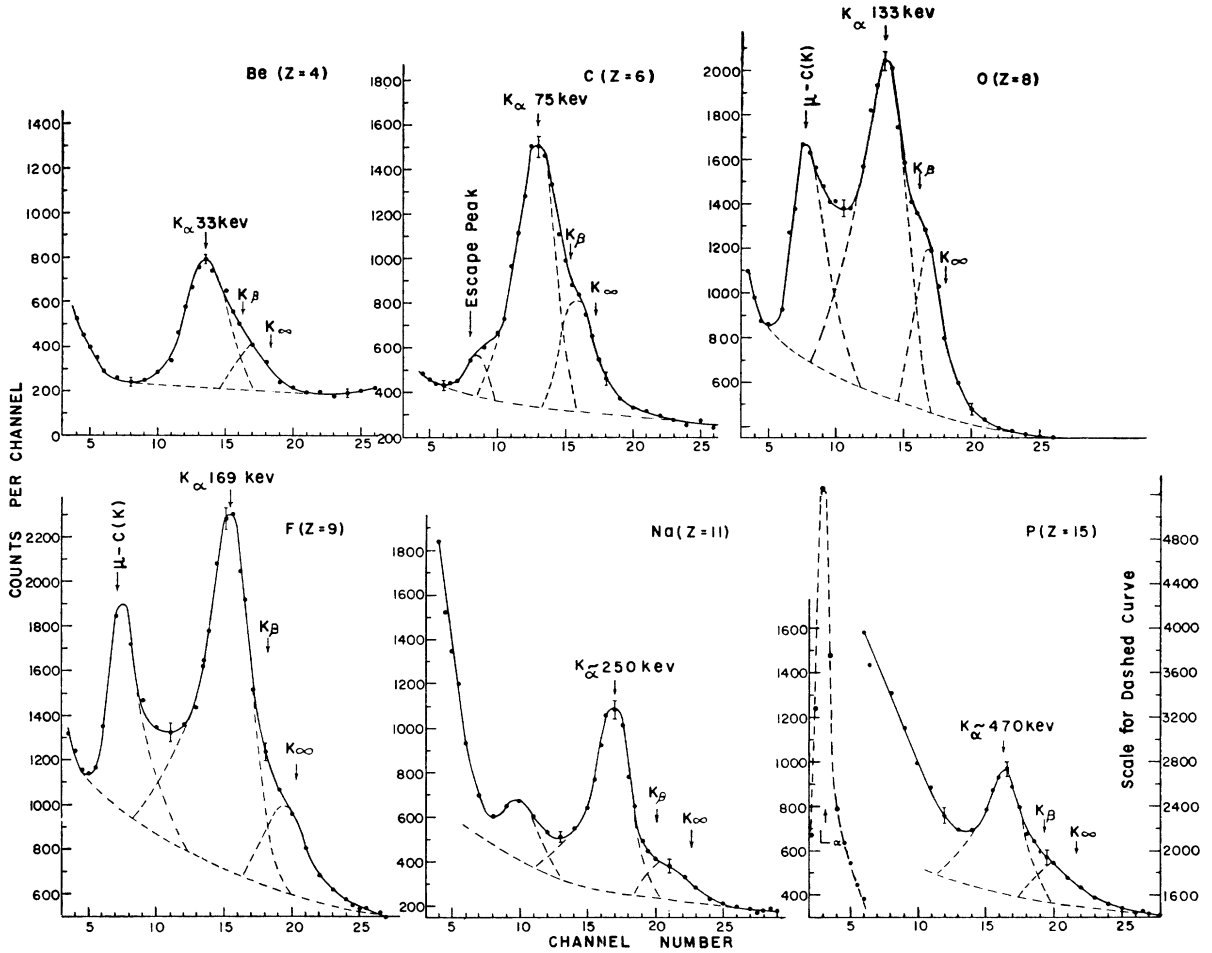

FIG. 6. Typical $\mu-K$ spectra. Each curve shown is normalized to the same number of stopped mesons. The $\mu-$C(K) contamination, well resolved in the O and F spectra, resulted from mesons stopping in the third counter of the meson telescope. The sharp rise at the low-energy end of the Na and P spectra is caused by L lines. The L peak of P is shown on a different scale (dashed curve). The positions at which the K_β and K_∞ should appear are indicated in each spectrum. Since the higher transitions are quite close in energy to the K_α line ($K_\beta \simeq 1.18 K_\alpha$), they are not clearly resolved and appear as a high energy bump.

III. EXPERIMENTAL RESULTS

A. $\mu-K$ Radiative Yields

The $\mu-K$ mesonic x-ray yields were measured for the elements $_3$Li through $_{19}$K. (By the K yield we mean the integrated yield of all the K-lines, $2p\rightarrow 1s$, $3p\rightarrow 1s$, $4p\rightarrow 1s$, etc.) The $\frac{1}{16}$-in. NaI crystal was used for Li and Be with their respective matching carbon targets, the $\frac{1}{2}$-in. NaI crystal for matching B, C, and N targets, and the 2-in. crystal for C and all higher-Z targets. Each element was run at least twice. Typical spectra for some of the $\mu-K$ lines are shown in Fig. 6. Since the pulse height selector did not have a sufficient number of channels to observe the detail desired, each spectrum was obtained by setting the p.h.s. to scan overlapping energy regions (usually three). These were then combined to give the complete spectrum. The curves of Fig. 6 are these composite curves. The outstanding features are the main peak due to the $2p\rightarrow 1s$ (K_α) transition and a high-energy tail from higher transitions. For the K series the higher transitions are not very clearly resolved, since the $3p\rightarrow 1s$ (K_β) transition is only 1.18 times the K_α energy. The situation is improved in the L series where $K_\beta \simeq 1.35 K_\alpha$. The contaminant K line from the carbon in the third counter is clearly seen in the spectra of oxygen and fluorine and can be subtracted off quite accurately. The corrected $\mu-K$ radiative yields are shown in Fig. 7. The largest contribution to the errors comes from uncertainties in backgrounds. In Table I are tabulated the energies of the various K transitions, the relative yields, and the ratio of the sum of higher transitions to the total radiative yield. This higher transition ratio is roughly constant, within the accuracy of the measurements, and is about 0.22. It was measured with an accuracy of about 10 to 20%. The absolute yield was also obtained by numerically calculating the solid angle, with absorption corrections, for one target, and by

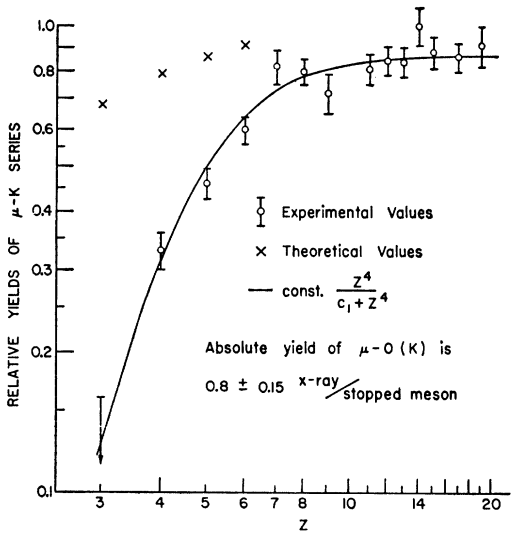

FIG. 7. $\mu-K$ series x-ray yield *vs* Z. The absolute total yield of oxygen is 0.80 ± 0.15 x-rays per captured meson. The experimental points have been fitted with the function, const$\cdot Z^4/(C_1+Z^4)$, suggested by Auger competition, where the constant is 0.86 and $C_1=450$ (in units of 1.3×10^{11} sec^{-1}). The Auger transition probability derived from this fit is about 300 times larger than the theoretical value. The crosses indicate the yield calculated from an initial $(2l+1)$ distribution of mesons captured in the $n=14$ level and their subsequent cascade process. The fall-off of the crosses at low Z is predominantly due to mesons passing through the $2s$ state from which they cannot radiate to the $1s$.

determining, in a separate experiment, the number of stopped mesons. This will be discussed in more detail in a subsequent paper on π-mesonic x-rays. The absolute oxygen $\mu-K$ yield was 0.8 ± 0.15 x-rays per stopped meson. This value is not as accurate as the corresponding value obtained for π mesons, since the smaller intensity muon beam was contaminated with an electron component. The relative values are, therefore, more accurate than the absolute values.

As seen in Fig. 7, for $Z\leqslant6$ the yield decreases rapidly with decreasing Z, presumably due to "Auger" competition. If this is true, and if we assume that the Auger transition probability is constant, then the radiative yield should behave approximately as

$$Y_R\simeq P(Z)[Z^4/(C_1+Z^4)]. \tag{1}$$

Here C_1 is the Auger transition probability in units of 1.3×10^{11} sec^{-1} (the radiative transition probability for $Z=1$). $P(Z)$, the population of the initial state, is an unknown but slowly varying function of Z. It depends on the distribution of the mesons at capture and on the subsequent cascade process. If Eq. (1) is plotted on log-log paper and $P(Z)$ is assumed constant, then C_1 is the only shape-dependent parameter. In Fig. 7 we have fitted Eq. (1) to the experimental points, assuming $P(Z)$ constant. The agreement is excellent. However, the Auger transition probability obtained by this match is about 300 times larger than that calculated by theory. This disagreement will be discussed further in Sec. IV.

B. $\mu-L$ Radiative Yields

The $\mu-L$ series yields were measured for the elements $_8$O through $_{19}$K. The $\frac{1}{16}$-in. NaI crystal was used for O, F, and Na and the $\frac{1}{2}$-in. crystal for Na and all

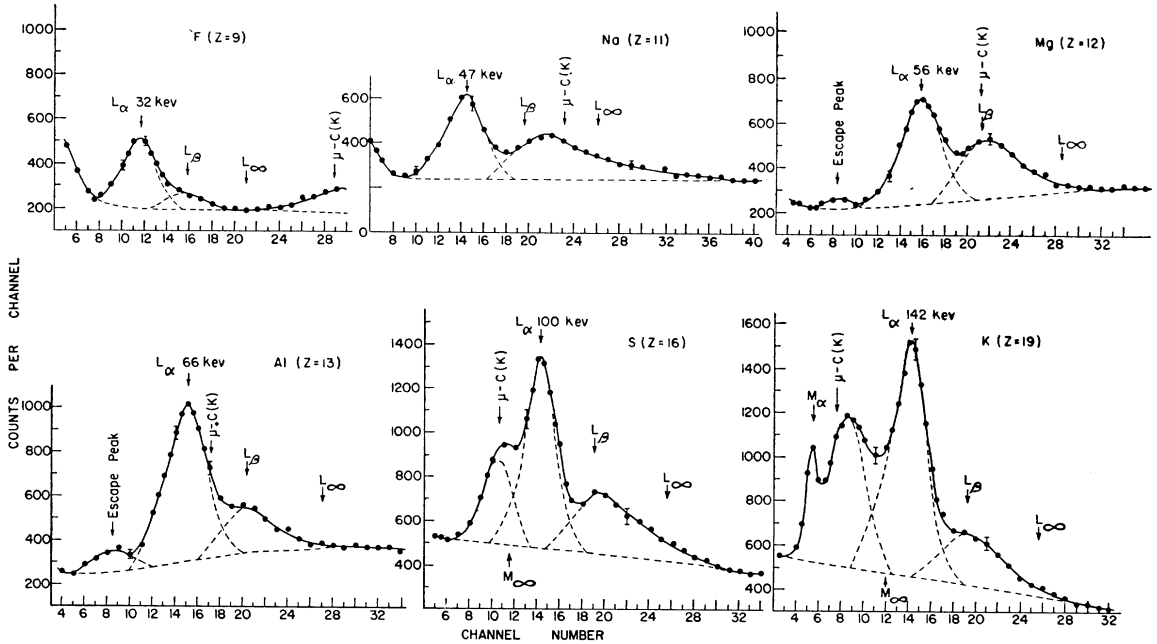

FIG. 8. Typical $\mu-L$ spectra. Each curve has been normalized to 3×10^5 stopped mesons. The higher transitions are more clearly resolved here since $L_\beta\simeq1.35L_\alpha$. Note the appearance of an M line in the potassium spectrum.

higher-Z targets. The complete radiative yield curve was measured twice. Typical spectra of some $\mu-L$ series x-rays are shown in Fig. 8, these again being composite curves. The outstanding features are the main peak due to the $3d\rightarrow 2p$ transition and the high-energy bump and tail from the higher transitions. The $\mu-K$ contaminant line from the carbon of the third counter is in evidence and is easily subtracted off since it is well resolved for some of the targets. Figure 9 shows the relative yields of the L series. Table II lists the energies, total relative yields, and the ratio of higher transitions to the total yield. The detector efficiency correction for this series is small and easily calculated since the highest energy line is only 142 kev. The yields are observed to decrease

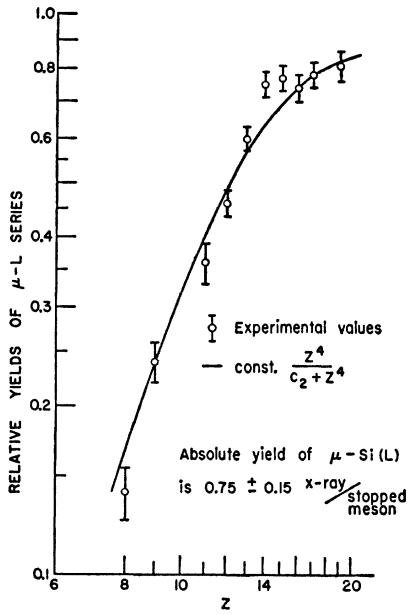

FIG. 9. $\mu-L$ series x-ray yield *vs* Z. The absolute total yield of silicon is 0.75 ± 0.15 x-rays per captured meson. The experimental points have been fitted with the function, const$\cdot Z^4/(C_2+Z^4)$, where the constant is 0.97 and $C_2=2\times10^4$ (in units of 1.34×10^{10} sec^{-1}). The Auger transition probability derived from this fit is about 30 times larger than the calculated value.

with decreasing Z starting around $Z\simeq13$. Again we have fitted a curve proportional to $Z^4/(C_2+Z^4)$ to the experimental points. In this case the fit is reasonably good for a value of the Auger transition probability which is about 30 times larger than the calculated value. The absolute yield of silicon is 0.75 ± 0.15 x-rays per stopped meson. The ratio of the sum of higher transitions to the total yield is observed to be roughly constant, within the accuracy of the measurements. It is about 0.25 to 0.30.

C. Capture in Chemical Compounds

It is of considerable interest to know with what relative probabilities mesons are captured by the various atoms of a compound. This could be useful,

TABLE I. Energies and yields of the $\mu-K$ series.

Element	Energy of $2p\rightarrow1s$ (kev)	Relative radiative yield[a]	Ratio of higher transition to total
$_3$Li	18.7	<0.16	
$_4$Be	33.3	0.33 ±0.03	0.22
$_5$B	52.1	0.46 ±0.035	0.22
$_6$C	75.0	0.60 ±0.04	0.20
$_7$N	102	0.82 ±0.07	0.23
$_8$O	133	0.80 ±0.05	0.21
$_9$F	168	0.72 ±0.07	0.18
$_{11}$Na	249	0.81 ±0.06	0.18
$_{12}$Mg	295	0.845±0.06	0.24
$_{13}$Al	~350	0.84 ±0.06	0.24
$_{14}$Si	~410	1.01 ±0.10	0.26
$_{15}$P	~470	0.88 ±0.07	0.28
$_{17}$Cl	~590	0.86 ±0.06	0.25
$_{19}$K	~730	0.91 ±0.09	0.27

[a] Total absolute yield of $\mu-O(K)=(0.80\pm0.15)$x-rays/stopped meson.

for example, in meson capture studies employing nuclear emulsions or bubble chambers filled with complex liquids. Fermi and Teller[1] (hereafter F-T), in studying the capture of negative mesons in matter, conclude that "in chemical compounds the probability of capture near the various atoms is roughly proportional to their atomic numbers." This simple Z-dependence is derived by assuming that the capture probability by each atom is proportional to the meson energy loss to the various atoms near zero energy.

Experiments, up to the present time, have either contradicted the F-T theory or have been too ambiguous to interpret simply. The first clear-cut experiment was that of Panofsky *et al.*[8] in which π^--mesons were absorbed by LiH and CH_2. In each case the theory predicts that about one-fourth of the incident mesons should be absorbed by H. No hydrogen capture was observed. This contradiction with the F-T theory has been explained by proposing that the initial neutral hydrogen π^--meson system, formed when π^- mesons

TABLE II. Energies and yields of the $\mu-L$ series.

Element	Energy of $3d\rightarrow2p$ (kev)	Relative radiative yield[a]	Ratio of higher transition to total
$_8$O	25	0.14±0.015	0.28
$_9$F	32	0.24±0.02	0.18
$_{11}$Na	47	0.36±0.03	0.23
$_{12}$Mg	56	0.46±0.025	0.20
$_{13}$Al	66	0.60±0.03	0.23
$_{14}$Si	77	0.75±0.04	0.31
$_{15}$P	88	0.77±0.04	0.35
$_{16}$S	100	0.74±0.04	0.40
$_{17}$Cl	113	0.78±0.04	0.37
$_{19}$K	142	0.81±0.05	0.30

[a] Total absolute yield of $\mu-Si(K)=(0.75\pm0.15)$x-rays/stopped meson.

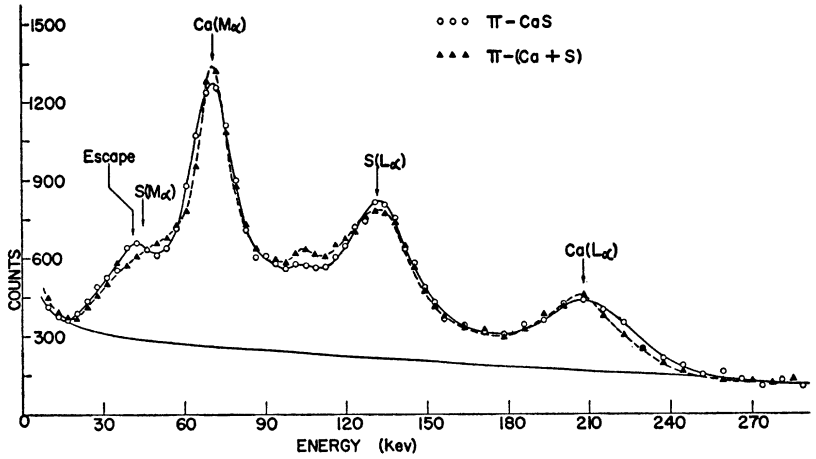

FIG. 10. X-ray spectra from π^--mesons captured in CaS and a mixture of Ca and S. The yields are the same to within 5%, indicating that meson capture in this compound is proportional to Z within 20%.

are captured by hydrogen, has a sufficiently long lifetime so that in subsequent collisions with the heavy elements in the lattice (i.e., Li or C) the meson is detached from its hydrogen partner and finally absorbed by the heavier atom. Experiments on the compound effect using photographic emulsion techniques suffer from the fact that while the gelatin is indeed a homogeneous mixture of C, N, H, and O, the AgBr crystals have macroscopic dimensions. This complicates the capture effect. In addition, the interpretation of a particular atomic capture in terms of prongs and stars and the ratio of alpha particles to protons is ambiguous, although the results are not in contradiction with the F-T theory. More recently Fafarman and Shamos[10] have studied the relative yields of mesonic x-rays from the capture of cosmic-ray μ mesons in dioxane ($C_4O_2H_8$). Their observed oxygen to carbon capture ratio was 0.33, which does not agree with the Z-dependence predicted by F-T (0.67). This experiment suffers from the very low intensity of cosmic-ray μ mesons and the character of the corrections involved in making absolute yield measurements. Because of these difficulties the results may be considered inconclusive.

Mesonic x-rays are an excellent tool in measuring the relative capture probabilities by the constituent atoms in compound. In principle one need only measure the relative radiative yields of some chosen transitions and then correct for nuclear absorption, Auger competition, detector efficiency, etc. In practice, however, the latter corrections, while perfectly straightforward, are large and the consequent errors can be large. It is, therefore, better, if possible, to compare the radiative yield from a compound with that of some sample which gives a simple Z-dependence. It can be shown that in a mechanical mixture of elements, each having the same weight as in the corresponding compound, the capture of mesons by the different constituent atoms is nearly proportional to Z. Thus for each compound under investigation one prepares, as a Z-dependence reference standard, a mixture of the same constituent elements. If, further, the geometries of the two are identical, no corrections need be made for x-ray absorption, detector efficiency, etc.

Using this method we have compared the π-mesonic x-ray yield from CaS with that from a mixture of pure calcium and sulfur. Figure 10 shows that the yields are identical to within about 5%. If we assume that the yield from each element in the compound goes as Z^n, then

$$\frac{(Y_{Ca}/Y_S)_{comp}}{(Y_{Ca}/Y_S)_{mix}}=\frac{(Z_{Ca}/Z_S)^n}{(Z_{Ca}/Z_S)}=\left(\frac{Z_{Ca}}{Z_S}\right)^{n-1}$$
$$=\left(\frac{20}{16}\right)^{n-1}=1.00\pm0.05. \quad (2)$$

Hence, $n\simeq1.0\pm0.2$. Thus for CaS, meson capture has a simple Z-dependence to within about 20%.

We have also compared the μ-mesonic x-ray yield from Al_2O_3 with that from a mixture of aluminum and water. In this case 1-mil sheets of aluminum were uniformly stacked within a cylinder of water. (It can be assumed that those mesons originally captured by the hydrogen in water will subsequently be lost to and absorbed by the oxygen.) The results, shown in Fig. 11, indicate that the yields are identical to within about 5%. Again assuming a Z^n dependence for each element in the compound, we get

$$\frac{(Y_{Al}/Y_O)_{comp}}{(Y_{Al}/Y_O)_{mix}}=\frac{\frac{2}{3}(Z_{Al}/Z_O)^n}{\frac{2}{3}(Z_{Al}/Z_O)}=\left(\frac{Z_{Al}}{Z_O}\right)^{n-1}$$
$$=\left(\frac{13}{8}\right)^{n-1}=1.00\pm0.05. \quad (3)$$

Hence, $n\simeq1.0\pm0.1$. Thus for both Al_2O_3 and CaS the meson capture probabilities are roughly proportional to Z, as predicted by the F-T theory.

We have not explicitly studied any other compounds.

[10] A. Fafarman and M. H. Shamos, Phys. Rev. **100**, 874 (1955).

However, we have indirect evidence from the radiative K and L series yield curves that mesons coming to rest in LiF are predominantly captured by the fluorine atoms. The radiative yields from fluorine were measured with this compound. The F-T theory predicts that three-fourths of the stopped mesons are captured by fluorine atoms and, therefore, the measured fluorine yield should be multiplied by the factor, 4/3. Doing this, however, gives an anomalously high yield for fluorine, putting it well above the smooth curve defined by its neighbors. Without the correction the fit is quite good (see Figs. 7 and 9 where the fluorine yield has not been corrected for lithium capture). The π-meson radiative yields show the same effect. Perhaps, when the Z's of elements in a compound differ by a large factor, the heavier elements capture a greater share than that alloted by a strict Z dependence. This problem should be examined further.

IV. DISCUSSION OF RESULTS

A conspicuous feature of the K and L μ-meson radiative yields is the rapid decrease in yield at lower Z's. This behavior is difficult to understand. The most reasonable explanation is to attribute this effect to Auger competition. However, the Auger transition probabilities needed to agree with the experimental results are 30 to 300 times larger than the theoretical values. These have been calculated by Burbidge and deBorde[11] and by deBorde[12] in a manner analogous to calculations of the electronic Auger effect. To a first approximation the Auger transition rates involve the same selection rules as dipole radiation, and deBorde gives formulas for the emission of electrons from the K and L shells for the meson transitions $(n_1,l_1)\rightarrow(n_2, l_1\pm1)$.

In an attempt to explain this discrepancy, we have investigated the effect of the initial capture distribution of the mesons and their subsequent cascade process on the radiative yield. Two different initial distributions of the mesons were examined. In both the mesons were assumed to be captured in the $n=14$ levels. In the first distribution the mesons were distributed among the available l substates in accordance with the statistical weights of the states, $(2l+1)$. The second distribution was chosen proportional to $(14)^l$, which is strongly peaked at large l and, therefore, favors circular orbits. Each distribution was then followed down through its cascade scheme using values of the Auger and radiative transition probabilities given by deBorde. His formulas show that the more likely Auger transitions are of the type $\Delta n=\Delta l=-1$. In calculating the cascade scheme we have neglected the transitions $(\Delta n=-1, \Delta l=+1)$ and $(\Delta n>1)$, except in the case of $l_1=0$, where $\Delta l=+1$ is the important transition. The $2s$ level is an exception since mesons passing through the $2s$ level cannot radiate to the $1s$ ground state and must necessarily undergo an Auger transition. Indeed, the cascade calculations show that the only practical way a meson can avoid making a K radiative transition in elements of $Z\geqslant3$ is by passing through the $2s$ level.

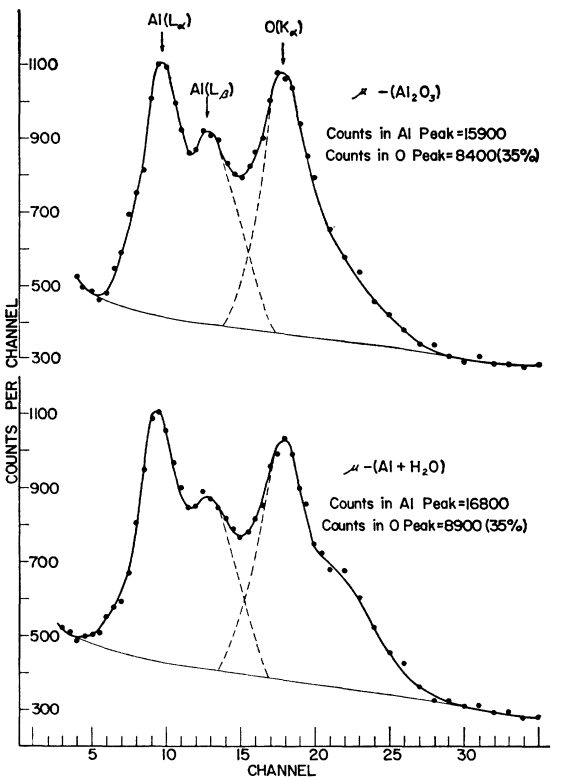

FIG. 11. X-ray spectra for μ^--mesons captured in Al_2O_3 and a mixture of Al plus H_2O. The yields are the same to within 5%. This indicates that meson capture in Al_2O_3 is proportional to Z to within about 10%.

In Fig. 7 the crosses give the calculated $\mu-K$ radiative yields for the $(2l+1)$ distribution. As can be seen, agreement with experiment is poor. The small decrease in radiative yield at low Z is the result of mesons passing through the $2s$ level. The $(14)^l$ distribution gives even poorer agreement as might be expected, since, favoring higher l values, it gives even fewer mesons passing through the $2s$ level.

The above might suggest that agreement with experiment could be improved by choosing initial distributions which favor the capture of mesons in low l states. However, such distributions appear to be ruled out by the following argument. As will be shown in a subsequent paper, some of the $\pi-L$ radiative yields are as large as 0.70 x-rays per stopped meson. If the reasonable assumption is made that π mesons which pass through $l=0$ states are absorbed by the nucleus, then, in order to avoid an appreciable depletion of mesons, we are led to the conclusion that the initial capture distribution must favor high l's. However, there is evidence that it cannot do this too strongly. As shown in Tables I and II, an appreciable amount of

[11] G. R. Burbidge and A. H. deBorde, Phys. Rev. **89**, 189 (1953).
[12] A. H. deBorde, Proc. Phys. Soc. (London) **67**, 57 (1954).

higher transitions was measured for both the $\mu-K$ and $\mu-L$ series and was quite independent of the target material. This is incompatible with an extreme distribution such as $(14)^l$. Therefore, we conclude that high-l states must be favored, but moderately.

Thus it appears that the observed discrepancy between experiment and the calculated Auger values cannot be simply explained by assumptions about the meson capture distribution and the subsequent cascade process. A more refined examination than that described in the foregoing produces only greater disagreement. For example, no account was taken of the depletion of the K and L electrons due to previous Auger transitions. Such depletion would clearly reduce Auger competition. Of course, it is possible that the observed decrease at low Z is the result of some mechanism other than Auger competition. We cannot think of any likely prospect. Whatever the mechanism, its Z dependence is similar to that of the Auger effect in view of the good fit of Eq. (1) to the experimental points.

PHYSICAL REVIEW VOLUME 105, NUMBER 5 MARCH 1, 1957

Nonradiative Absorption of Positive Pions by Deuterons at 118 Mev*†

CHARLES ERWIN COHN‡
The Enrico Fermi Institute for Nuclear Studies, The University of Chicago, Chicago, Illinois
(Received November 29, 1956)

The reaction $\pi^+ + d \rightarrow p + p$ was studied at a center-of-mass pion energy of 118±2 Mev, using scintillation counters and a liquid deuterium target. The angular distribution was given by $d\sigma/d\Omega \propto A + \cos^2\theta$, with $A = 0.216 \pm 0.033$, while the total cross section was 12.09±0.93 mb. The total cross section for the inverse pion production reaction was calculated from detailed balancing as 3.10±0.24 mb. These results are compared with other work.

I. INTRODUCTION

THE pion production reaction $p+p \rightarrow \pi^+ + d$ and the inverse nonradiative pion absorption reaction $\pi^+ + d \rightarrow p + p$ have been investigated by many workers, and data are available on total cross sections and angular distributions at center-of-mass pion energies up to 156.5 Mev. Most of the data has been compiled by Rosenfeld[1] with later work reported by Crawford and Stevenson,[2] Meshcheryakov *et al.*,[3,4] and Rogers and Lederman.[5] The work on total cross sections for the higher energies is shown on Fig. 1, while that on angular distribution is plotted on Fig. 2. The data on Fig. 1, both from production and absorption measurements, are plotted in terms of the production cross section; the absorption cross section being related to the former by a simple detailed balancing relationship.[6]

This paper describes measurements of the absorption reaction at a pion c.m. energy of 118±2 Mev. These were done mainly to test the hypothesis of Meshcheryakov that the angular distribution parameter A is substantially constant between 70 and 160 Mev. However, the results of Stadler[7] suggest a rise with energy in this region. This question is of special interest because the $(\frac{3}{2},\frac{3}{2})$ pion-nucleon resonance would be expected to take effect in this region.

The present results are in substantial agreement with Meshcheryakov. The implications are discussed in terms of the phenomenological theory.

II. THEORY

At present, the best interpretation and correlation of these data are given by a phenomenological theory of Gell-Mann and Watson,[8] who assume that the pion participates in these reactions only in S or P angular momentum states. With this assumption, it is possible to enumerate the quantum states between which the reaction may take place. The result is shown in Table I,

TABLE I. Possible processes for reaction $\pi^+ + d \rightleftarrows p + p$ with pion in S or P states.

Pion angular momentum state	Total J for pion-deuteron system	$p+p$ state	Cm angular dist. of reaction prod. for isolated case
S	1	$^3P_1$	isotropic
P	0	$^1S_0$	isotropic
P	2	$^1D_2$	$\frac{1}{3}+\cos^2\theta$

* Research supported by a joint program of the Office of Naval Research and the U. S. Atomic Energy Commission.
† Based on a thesis submitted to the Faculty of the Department of Physics, the University of Chicago, in partial fulfillment of the requirements for the Ph.D. degree.
‡ Present address: Argonne National Laboratory, P. O. Box 299, Lemont, Illinois.
[1] A. H. Rosenfeld, Phys. Rev. **96**, 139 (1954).
[2] F. S. Crawford and M. L. Stevenson, Phys. Rev. **97**, 1305 (1955).
[3] M. G. Meshcheryakov *et al.*, Doklady Akad. Nauk S.S.S.R. **100**, 673 (1955).
[4] M. G. Meshcheryakov *et al.*, Doklady Akad. Nauk S.S.S.R. **100**, 677 (1955).
[5] K. C. Rogers and L. M. Lederman, Nevis Cyclotron Laboratories Report 25 (unpublished).
[6] W. B. Cheston, Phys. Rev. **83**, 1118 (1951).
[7] H. L. Stadler, Phys. Rev. **96**, 496 (1954).
[8] M. Gell-Mann and K. M. Watson, Annual Review of Nuclear Science (Annual Reviews, Inc., Stanford, 1954), Vol. 4, p. 219.